Optimization of Bioethanol Production from *Chlorella vulgaris* with Ca^{2+}, Mg^{2+}, and Zn^{2+} Ion Supplementation via Separate Hydrolysis and Fermentation Using Response Surface Methodology

Muhammad Fakhrudin Zukhri[a], Afan Hamzah[a*], Muhamad Khoirul Anam[b]

[a]*Department of Industrial Chemical Engineering, Institut Teknologi Sepuluh Nopember, Surabaya, 60111, Indonesia*
[b]*Department of Development Studies, Institut Teknologi Sepuluh Nopember, Surabaya, 60111, Indonesia*
Corresponding author: afan@its.ac.id

Abstract

Indonesia, with its wealth of natural resources, has the potential to develop bioethanol as an alternative to diminishing fossil energy sources. Third-generation bioethanol is a form of renewable energy and an environmentally friendly fuel derived from non-conventional biomass resources, particularly from microorganisms such as algae and cyanobacteria. This study focuses on optimizing the bioethanol production process from the microalga Chlorella vulgaris using the Separated Hydrolysis and Fermentation (SHF) method, with the addition of Ca^{2+}, Mg^{2+}, and Zn^{2+} ions to enhance bioethanol content and concentration. The research procedure includes raw material pretreatment, acid hydrolysis, liquefaction, saccharification, fermentation, and distillation. The distillate samples are analyzed for bioethanol concentration using a refractometer and bioethanol concentration. The effect of added medium components on the fermentation process is statistically analyzed using Analysis of Variance (ANOVA) in MINITAB Statistical Software and Response Surface Methodology (RSM) in DESIGN EXPERT 13. Statistical optimization of the fermentation process is performed using Central Composite Design (CCD). ANOVA analysis reveals that Mg^{2+}, Ca^{2+}, and Zn^{2+} significantly influence bioethanol content (%) and concentration (g/L), with a P-value <0.0001. Optimization results indicate an optimal content of 17.087% with a concentration of 165.592 g/L, achieved with the addition of Ca^{2+} at 164.755 ppm, Mg^{2+} at 146.279 ppm, and Zn^{2+} at 38.516 ppm.

Keywords: Bioethanol; Chlorella vulgaris; Separated hydrolysis and fermentation

1. Introduction

The increasing energy consumption and environmental issues such as air pollution and global warming resulting from the combustion of fossil fuels have necessitated the search for bio-based resources from renewable fuels [1]. One type of biofuel that is currently being progressively developed in Indonesia is bioethanol. Unfortunately, the rate of bioethanol utilization in Indonesia has not been followed by the same rate of biodiesel development, despite the substantial potential of bioethanol to match biodiesel. This is evident from the issuance of Ministerial Regulation No. 12/2015, which regulates the use of bioethanol as a biofuel, E5 (5% bioethanol and 95% gasoline) by 2020. Initially, first-generation bioethanol was produced from consumable biomass such as potatoes, corn, wheat, barley, sugarcane, sugar beets, and vegetable oils, which could replace the use of fossil fuels and reduce CO_2 emissions to the environment [2]. However, the use of first-generation fuel sources can lead to food crises. To address this issue, second-generation bioethanol is produced from non-edible lignocellulosic materials, such as agricultural waste or wood residues [3][4]. However, the seasonal dependency on raw materials remains a major drawback of second-generation biofuels. Third-generation bioethanol, produced from algae, provides an effective renewable alternative for bioethanol production, overcoming the shortcomings of both first and second-generation bioethanol [5].

Microalgae and macroalgae are considered among the most promising bio-feedstocks for bioethanol production. These organisms obtain nutrients from energy provided by sunlight, water, minerals, and CO_2. In general, bioethanol production can be carried out using *Separated Hydrolysis and Fermentation* (SHF) or *Simultaneous Saccharification and Fermentation* (SSF). SHF is a conventional method in which the hydrolysis process is first conducted to produce monosaccharide sugars, followed by the fermentation process. In contrast, in the SSF method, enzymes and yeast are combined in a single reactor, allowing glucose to be rapidly converted into ethanol. Fermentation

is typically carried out using the microorganism *Saccharomyces cerevisiae*, as this species has a high survival rate and is capable of producing ethanol in large quantities. *S. cerevisiae* produces ethanol by fermenting hexose sugars but is unable to ferment pentose sugars. This microorganism grows optimally at a temperature range of 25ºC – 30ºC and prefers acidic conditions within a pH range of 4–5 [6].

During fermentation, the production of bioethanol from microalgae requires enhanced yeast cell stability during the fermentation process [7]. The effect of adding Mg^{2+}, Ca^{2+}, and Zn^{2+} ions on bioethanol production refers to how the introduction of these metal ions influences the efficiency and content of bioethanol during fermentation. In many fermentation processes, particularly those involving Saccharomyces cerevisiae, the addition of mineral ions like magnesium (Mg^{2+}) and calcium (Ca^{2+}) can enhance the metabolic activity of yeast and improve the fermentation process and Zn^{2+} ions played a supporting role in enhancing enzymatic activity [8]. Demiray et al. (2018) evaluated the effects of nitrogen sources and several inorganic ions/metal salts (K^{+}, Mg^{2+}, Ca^{2+}, Zn^{2+}) on ethanol production from pomegranate peel using the well-known yeast *Saccharomyces cerevisiae* and the pentose-fermenting yeast *Pichia stipitis*. In pomegranate peel medium without supplementation, the ethanol concentration was 3.85 g/L. Ethanol content increased by up to 44.9% with the addition of $MgSO_4 \cdot 7H_2O$, KH_2PO_4, $CaCl_2$, and $ZnSO_4$. However, this significant effect was not observed in *Pichia stipitis*, as no substantial changes in ethanol production were detected even with the addition of yeast extract, peptone, or metal salts to the medium [9].

As a summary of the reported bibliographic data, we conclude the important role of mineral supplementation as nutrients in enhancing cell growth during the fermentation process, which significantly improves ethanol production content. Therefore, this study aims to optimize the effect of Mg^{2+}, Ca^{2+}, and Zn^{2+} ion supplementation in the fermentation medium for bioethanol production from Chlorella vulgaris through Separated Hydrolysis and Fermentation (SHF) using Response Surface Methodology, which has not been previously reported.

2. Materials and Method

2.1. Materials

The materials used in this study include H_2SO_4 2N, HCl 1N, enzim α-amilase, enzim β-amilase, Ammonium Sulfat ($(NH_4)_2SO_4$), Kalium Monofosfat (KH_2PO_4), yeast extract saccharomycess cerevisiae, buffer sitrat, $CaCl_2$, $MgSO_4.7H_2O$, $ZnSO_4.7H_2O$.

2.2 Method

2.2.1 Pretreatment

The pretreatment process aims to enhance the growth population of *Chlorella vulgaris* microalgae. Initially, 500 ml of algae seed culture is mixed with 500 ml of freshwater and then transferred to a culture medium. In this medium, the algae grow with the support of oxygen supply and sunlight for photosynthesis. After being cultured for 7 days, the algae reach their rapid growth phase. At this stage, the algae are harvested and filtered to separate the algal biomass from water. The biomass is then dried to reduce moisture content and subsequently ground using a 100-mesh.

2.2.2 Acid Hydrolysis and Enzymatic Saccharification

The acid hydrolysis and saccharification of *Chlorella vulgaris* follow the method outlined in prior research. Acid hydrolysis was performed using 10% H_2SO_4 2N, autoclaved at 121ºC for 45 min and neutralized with citrate buffer until the pH reached [10]. liquefaction and saccharification processes were conducted according to Soeprijanto, et al., (2021), After hydrolysis, liquefaction was carried out by adding 1,5 v/v enzyme α-amilase, along with 40 mg/L $CaCl_2$ as an enzyme stabilizer, followed by heating at 90ºC at 2 hours. The liquefied product was cooled to 60°C, and the pH was adjusted to 4.5–5 by adding 1N HCl. Subsequently, saccharification was performed by adding 5 ml of β-amylase enzyme and heating at 65°C for 4 hours.

2.2.3 Fermentation

The bioethanol fermentation process was conducted following Agwa, et al., (2017). The fermentation was carried out in 250 ml Erlenmeyer flasks as reactors. The algal hydrolysate was supplemented with 2 g/L Ammonium Sulfate ($(NH_4)_2SO_4$) 2g/L, Potassium Monophospate (KH_2PO_4) 1g/L, and 2 g/L Saccharomyces cerevisiae yeast extract. The addition of mineral ions in the fermentation medium followed the variables outlined in the design of experiments,

where Ca^{2+} was sourced from$CaCl_2$, Mg^{2+} from $MgSO_4.7H_2O$, and Zn^{2+} from $ZnSO_4.7H_2O$. fermentation medium was sterilized at 121°C for 25 minutes.

2.2.4 Distillation

The fermentation product was distilled using a 250 ml distillation apparatus set at 78°C, which corresponds to the boiling point of bioethanol.

2.2.5 Bioethanol Quality Analysis anExperimental Design

The distilled samples were analyzed using a refractometer to determine bioethanol content (%) and bioethanol concentration (g/L). The bioethanol concentration for each sample was determined using the following equation:

$$Bioethanol\ Concentration\ (g/L) = 10\ x\ EtOH\ Content\ x\ \rho \quad (1)$$

where ρ = ethanol density (g/ml)

$$Bioethanol\ Density\ (g/ml) = \frac{(b-a)}{(c-a)} x \rho_{aquadest} \quad (2)$$

Where; a = weight of empty pycnometer (g), b = weight of pycnometer+bioethanol (g), c = weight of pycnometer+aquades (g), and $\rho_{aquadest}$ = 0.9662 g/ml

2.2.5 Experimental Design

The effect of medium component addition during the fermentation process was statistically analyzed using Analysis of Variance (ANOVA) with MINITAB Statistical Software and Response Surface Methodology (RSM) using DESIGN EXPERT 13 software. Statistical optimization of the fermentation process was conducted using Central Composite Design (CCD). Response Surface Methodology (RSM) based on Central Composite Design (CCD) was employed to optimize bioethanol production. Independent variables selected for the optimization of bioethanol fermentation, specifically the concentrations of Ca^{2+}, Mg^{2+}, and Zn^{2+} ions in the fermentation medium shown in table 1. The fermentation parameters that significantly influence bioethanol content were selected based on the experimental data employed to investigate the effects of Ca^{2+}, Mg^{2+}, and Zn^{2+} on bioethanol production shown in table 2.

Table 1. Independent-dependent variables and boundary values.

Factor	Name	Units	Change	Type	SubType	Minimum	Maximum	Coded Low	Coded High
a	Ca^{2+}	ppm	Hard	Numeric	Continuous	0.0000	200.00	-1 ↔ 0.00	+1 ↔ 200.00
B	Mg^{2+}	ppm	Easy	Numeric	Continuous	0.0000	150.00	-1 ↔ 0.00	+1 ↔ 150.00
C	Zn^{2+}	ppm	Easy	Numeric	Continuous	0.0000	50.00	-1 ↔ 0.00	+1 ↔ 50.00

Table 2. Design of experiment.

Group	Run	a:Ca^{2+}	B:Mg^{2+}	C:Zn^{2+}
		ppm	ppm	ppm
4	12	0	0	0
4	10	0	120	50
4	11	0	150	20
2	6	90	60	30
2	4	90	150	0
2	5	90	150	50
1	1	100	0	30
1	2	100	90	20

1	3	100	150	50
5	15	120	0	50
5	13	120	90	30
5	14	120	120	0
3	7	200	60	50
3	8	200	60	20
3	9	200	150	20

Analysis of Variance (ANOVA) is used to determine the significance of each factor in bioethanol production using linear, interactive, and quadratic approaches, which are represented by the following second-order quadratic equation:

$$Y = \beta_0 + \sum_{i=1}^{3} \beta_i x_i \sum_{i=1}^{3} \sum_{j=i+1}^{4} \beta_{ij} x_i x_j + \sum_{4}^{i=1} \beta_{ii} x_i^2 \quad (3)$$

Where Y represents the bioethanol content (%), β_0 is the central point value, and β_i, β_{ij}, and β_{ii} are the linear, interactive, and quadratic coefficients, respectively. Meanwhile, x_i and x_j represent the independent factors [11].

3. Results and Discussion

3.1. The Effect of Mineral Addition on Bioethanol Concentration

Table 4.1 presents the results of the effect of mineral additions, including Ca^{2+}, Mg^{2+}, and Zn^{2+} ions, on bioethanol production, measured in terms of solution concentration (g/L) and ethanol (EtOH) content as a percentage.

Table 3. Effect of mineral addition on bioethanol concentration.

Group	Run	Factor 1	Factor 2	Factor 3	Response 1	Response 2
		a:Ca^{2+}	B:Mg^{2+}	C:Zn^{2+}	Concentration	EtOH Content
		ppm	ppm	ppm	g/L	%
1	1	100	0	30	80.73	8.22
1	2	100	90	20	87.67	8.94
1	3	100	150	50	156.58	16.15
2	4	90	150	0	136.49	14.03
2	5	90	150	50	150.26	15.48
2	6	90	60	30	84.47	8.62
3	7	200	60	50	153.6	15.83
3	8	200	60	20	61.98	6.29
3	9	200	150	20	158.31	16.33
4	10	0	120	50	88.74	9.05
4	11	0	150	20	110.62	11.32
4	12	0	0	0	50.13	5.08
5	13	120	90	30	82.87	8.44
5	14	120	120	0	82.33	8.39
5	15	120	0	50	125.3	12.78

The experiment was divided into several runs with varying concentrations of added minerals. Response 1, which refers to solution concentration, ranged from 61.98 g/L to 158.31 g/L, while Response 2, which refers to ethanol content, ranged from 6.29% to 16.35%. The addition of Ca^{2+}, Mg^{2+}, and Zn^{2+} ions significantly affected the quality of the produced bioethanol, as measured by solution concentration (g/L) and ethanol content (%). Previous studies Alminderej et al. (2022), the variation in Ca^{2+} concentration in the fermentation medium exhibited a significant impact on bioethanol production. At 0.2 g/L Ca^{2+}, ethanol content was 33.4 ± 0.8 g/L, while increasing the concentration to 0.4 g/L resulted in the highest ethanol production of 41.5 ± 0.85 g/L, indicating the optimal role of Ca^{2+} in enhancing

Saccharomyces cerevisiae cell stability and metabolic activity. However, at 1 g/L Ca^{2+}, ethanol production declined to 39.9 ± 0.9 g/L, possibly due to toxicity effects disrupting osmotic balance and enzymatic activity. Therefore, 0.4 g/L Ca^{2+} was identified as the optimal concentration, as further increases could potentially hinder fermentation efficiency [12]. Kounbesiou et al. (2010) conducted a 7-day fermentation using *Saccharomyces cerevisiae* with the addition of Mg^{2+} ions at concentrations of 0, 0.1, 0.2, 0.4, 0.6, 0.8, and 1.0 g/L. The results indicated that the maximum bioethanol concentration of 17 g/L was achieved at 1.0 g/L Mg^{2+} supplementation. Furthermore, the findings demonstrated a positive correlation between Mg^{2+} ion addition and bioethanol production, suggesting its role in enhancing yeast metabolism and fermentation efficiency[13]. Wan et al. (2014) reported that yeast cells supplemented with 0.03 g/L Zn^{2+} exhibited growth initiation at 23 hours post-inoculation, which was 12 hours earlier than the control culture. Zinc supplementation significantly shortened the fermentation time to 45 hours, while the highest biomass obtained was 3.5 g/L, representing a 15% increase compared to the control. Although zinc addition had minimal impact on ethanol titer, the shortened fermentation time resulted in an ethanol productivity of 1.096 g/h, which was 30.8% higher than the control. These findings highlight the role of zinc in accelerating yeast metabolism and fermentation efficiency, leading to enhanced overall productivity [14].

Mg^{2+} ions played a crucial role in enhancing fermentation efficiency, as seen in run 3 and run 9, where the concentration and ethanol content reached their highest levels when Mg^{2+} was added at the optimal concentration in combination with Ca^{2+} and Zn^{2+}. Souza, et al., (2016) have reported that Mg^{2+} enhances yeast metabolic activity, stabilizes cell membranes, and improves ethanol content in *Saccharomyces cerevisiae* fermentation. Our findings align with these results, further confirming the necessity of Mg^{2+} supplementation for efficient bioethanol production [15]. The addition of Ca^{2+} also supported high bioethanol production, as seen in run 7 and run 9, where the combination with Mg^{2+} and Zn^{2+} resulted in ethanol content as high as 16.33%. Conversely, the absence or decrease in Mg^{2+} concentration resulted in a significant reduction in content, as seen in run 1 and run 8. Zn^{2+} ions played a supporting role in enhancing enzymatic activity, but an excess concentration without the presence of other ions did not show significant improvement, as in run 12. Previous studies Rachman, et al., (2016) have demonstrated that Zn^{2+} metal ions enhance yeast cell tolerance to ethanol-induced stress, as evidenced by higher cell viability following ethanol exposure. Although Zn^{2+} supplementation exerts a beneficial effect, excessive concentrations have been reported to negatively impact cell viability. The improvement in cell viability is expected to contribute to increased ethanol production, as a higher number of metabolically active yeast cells are available to convert sugars into ethanol. Overall, a balance between Ca^{2+}, Mg^{2+}, and Zn^{2+} ions is required to optimize bioethanol production, with Mg^{2+} acting as the dominant factor in enhancing the efficiency of sugar conversion to ethanol. Magnesium is a cofactor necessary for the activity of several enzymes involved in glycolysis and other fermentation processes. The presence of Mg^{2+} ions can accelerate the fermentation rate and improve sugar-to-ethanol conversion efficiency, resulting in higher bioethanol levels [16]. Calcium plays a role in stabilizing cell membranes and enzyme activity. The addition of Ca^{2+} ions can improve cell viability and metabolic efficiency during fermentation, leading to increased bioethanol production [17]. Zinc is essential for the function of dehydrogenase enzymes and other enzymes involved in energy metabolism [18]. The addition of Zn^{2+} can enhance enzymatic activity and support yeast cell growth, ultimately contributing to increased ethanol production [19].

3.2. Model Equation

The second-order polynomial model obtained in this study describes the relationship between independent variables and bioethanol production as the response variable. This model includes linear components, variable interactions, and quadratic effects, enabling a more detailed analysis of the contribution of each factor and their interactions to the efficiency of bioethanol production[20]. The bioethanol production results were statistically analyzed using the second-order polynomial model with the following equation:

$$Y = 77.97 + 5.30X_1 + 36.14X_2 + 36.81X_3 + 22.74X_1X_2 + 27.45X_1X_3 - 28.02X_2X_3 + 1.84{X_1}^2 + 19.47{X_2}^2 + 8.14{X_3}^2 \quad (4)$$

The model coefficients include variables a, b, and c, which are the linear coefficients for the independent variables, while aB, aC, and BC are the interaction coefficients, and a^2, b^2, and c^2 are the quadratic coefficients. Model

validation was evaluated using the correlation coefficient (R^2), adjusted determination coefficient (Adj-R^2), and adequate precision [21].

Table 4. ANOVA analysis for the quadratic model.

Source	Term df	Error df	F-value	p-value	
Whole-plot	2	2.02	0.2652	0.7902	not significant
a-Ca^{2+}	1	2.04	0.5618	0.5305	
a^2	1	1.99	0.0387	0.8622	
Subplot	7	3.00	1137.55	< 0.0001	significant
B-Mg^{2+}	1	3.00	3093.78	< 0.0001	
C-Zn^{2+}	1	3.00	2203.41	< 0.0001	
aB	1	3.00	323.19	0.0004	
aC	1	3.00	817.32	< 0.0001	
BC	1	3.01	786.05	< 0.0001	
B^2	1	3.00	347.71	0.0003	
C^2	1	3.00	82.03	0.0028	

Table 5. Factor coefficients.

Source	Coefficient Estimate	Standard Error	VIF
Intercept	77.97	5.95	
Whole-plot Terms:			
a-Ca^{2+}	5.30	7.07	1.01
a^2	1.84	9.34	1.00
Subplot Terms:			
B-Mg^{2+}	36.14	0.6498	1.71
C-Zn^{2+}	36.81	0.7841	2.56
aB	22.74	1.26	2.79
aC	27.45	0.9601	1.52
BC	-28.02	0.9994	2.23
B^2	19.47	1.04	1.51
C^2	8.14	0.8986	1.32

Table 6. Model data.

Std. Dev.	10.12	**R^2**	0.9993
Mean	107.34	**Adjusted R^2**	0.9967
C.V. %	9.43		

The ANOVA analysis results in Table 4, the quadratic model is highly significant ($p < 0.0001$), which indicates a strong relationship between the independent variables and the response variable. The most significant variable is B-Mg^{2+}, as it has the highest F-value (3093.78) and a p-value < 0.0001, confirming its strong effect on the model. Other significant factors include C-Zn^{2+}, aB, aC, BC, B^2, and C^2, all of which have p-values less than 0.05, indicating a statistically significant impact [22]. Moreover, the coefficient of determination (R^2) is 0.9993. Similarly, the adjusted coefficient of determination (Adj-R^2) is 0.9967. Therefore, the obtained results confirm that both models are significant ($p < 0.05$). Additionally, the very low coefficient of variation (CV < 10%) indicates a high level of precision and good reliability of the experimental values. Table 5 presents the coefficient estimates for the factors in the experimental model, along with standard errors and Variance Inflation Factors (VIF). The intercept has a coefficient estimate of 77.97 with a standard error of 5.95. In the whole-plot section, the a-Ca^{+} coefficient is 5.30 with a standard error of 7.07 and a VIF of 1.01, while the a^2 coefficient is 1.84 with a standard error of 9.34 and a VIF of 1.00. Both factors show low VIF values, indicating the absence of significant multicollinearity. In the subplot section, the B-Mg^{2+} factor has a

coefficient estimate of 36.14 with a standard error of 0.6498 and a VIF of 1.71, while the C-Zn^{2+} factor has a coefficient estimate of 36.81 with a standard error of 0.7841 and a VIF of 2.56. Interaction factors such as aB and aC have coefficient estimates of 22.74 and 27.45 with standard errors of 1.26 and 0.9601, respectively, and VIFs of 2.79 and 1.52. The BC interaction factor has a coefficient estimate of -28.02 with a standard error of 0.9994 and a VIF of 2.23. The quadratic factors B^2 and C^2 have coefficient estimates of 19.47 and 8.14 with standard errors of 1.04 and 0.8986, respectively, and VIFs of 1.51 and 1.32. Table 6 shows the standard deviation (Std. Dev.) of 10.12 with a mean of 107.34, and the Coefficient of Variation (C.V.) is 9.43%. The R^2 value of 0.9993 and the Adjusted R^2 value of 0.9967 indicate an excellent fit of the model with the experimental data. These findings underscore the dominant role of Mg^{2+} and Zn^{2+} in bioethanol production, with their individual and interactive effects playing a critical role in optimizing the fermentation process.

3.3. Model Accuracy Graph

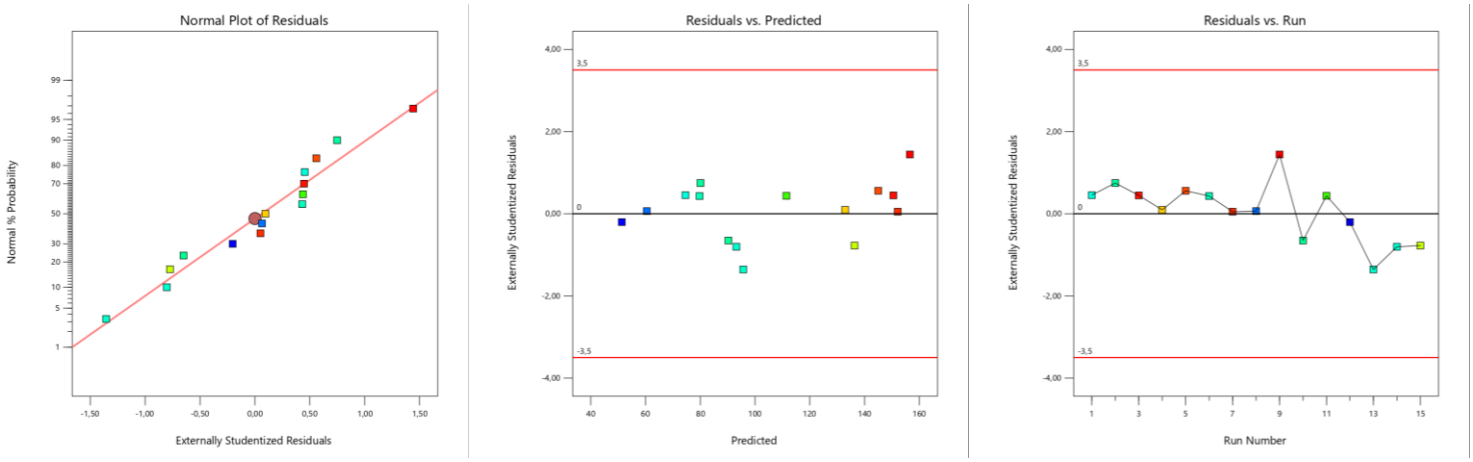

(a) (b) (c)

Figure 1. Model accuracy graphs and normal plot of residuals (a); Grafik Nilai residuals vs. predicted values (b); Predicted Values and residuals vs. experimental deviation graph (c).

These graphs provide insights into the validity of the assumptions in the regression model used to predict bioethanol production outcomes. Based on Figure 1(a), the normal plot of residuals indicates that the majority of points are distributed around the diagonal line, suggesting that the residuals follow a normal distribution. However, there are a few points that deviate from the line, indicating minor deviations from the normality assumption, although these are not significant [23]. These findings suggest that the normality assumption of residuals in this regression model is largely satisfied. In Figure 1(b), the externally studentized residuals are dispersed around the zero line. The distribution of these points does not show any specific pattern, indicating no signs of heteroscedasticity or significant issues with the assumption of linearity. This random dispersion suggests that the regression model does not suffer from heteroscedasticity, and it is expected to be suitable for predicting data with consistent variability across the entire range of predicted values. Figure 1(c) demonstrates that the residuals are evenly distributed around the zero line without any clear systematic pattern. This indicates the absence of autocorrelation in the residuals, meaning the data does not exhibit serial dependence or trends related to the sequence of data collection. These findings suggest that the experimental measurements were conducted consistently and that there is no bias caused by the order of the experiments.

3.4. 3D Graphs and Contour Plots

Optimization using the Response Surface Method (RSM) involves three main steps: statistically designing experiments, estimating coefficients in the mathematical model, and predicting responses while checking the adequacy of the model ($Y = f(x_1, x_2, x_3, ..., x_n)$), where Y represents the system response, and X_n are the action factors referred to as factors [24]. Graphical representations of the model are an effective method for determining the optimal location. Two types of graphs that can be used include the response surface in three dimensions (Figures 4.5a, 4.6a, and 4.7a) and contour plots, which are projections of the surface onto a flat plane and are represented as lines of constant response

(Figures 4.5b, 4.6b, and 4.7b). Each contour line corresponds to a specific surface elevation. In these graphs, the response is displayed as a function of two factors [25].

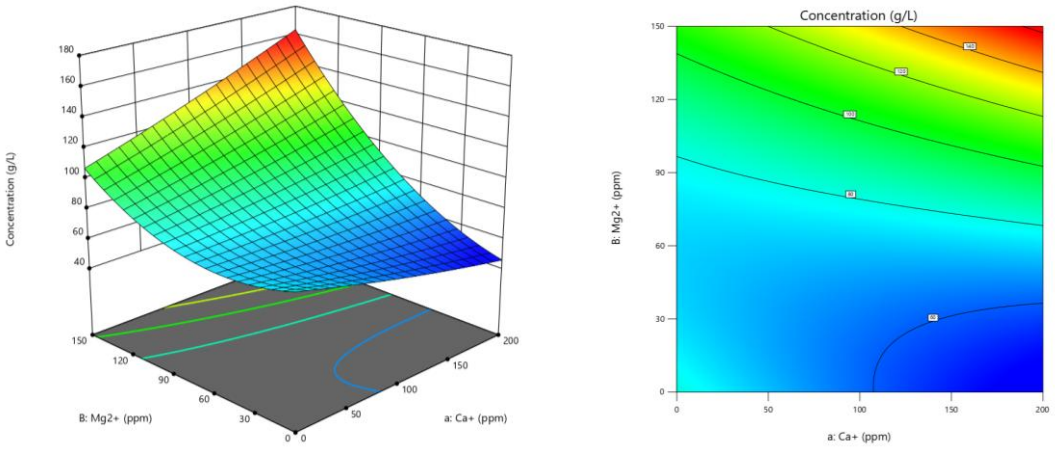

(a) (b)

Figure 2. Response surface for the addition of Mg^{2+} and Ca^{2+} ions on bioethanol concentration.

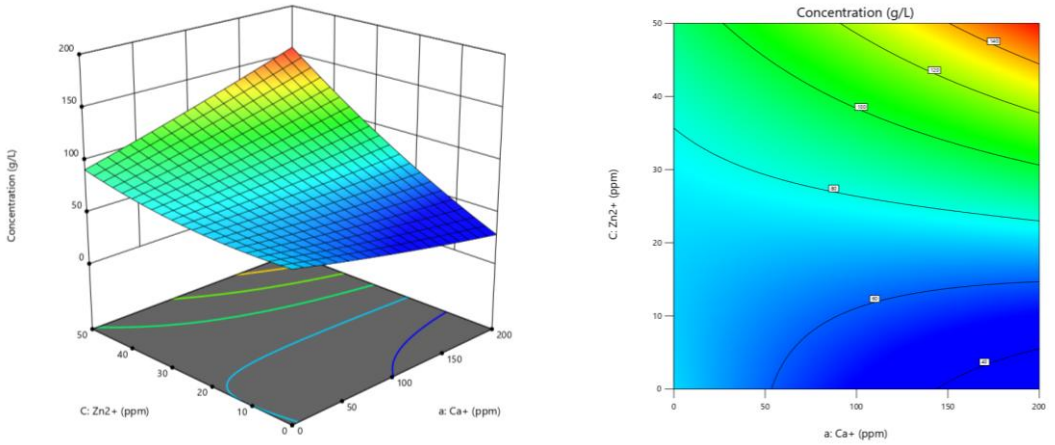

(a) (b)

Figure 3. Response surface for the addition of Zn^{2+} and Ca^{2+} ions on bioethanol concentration.

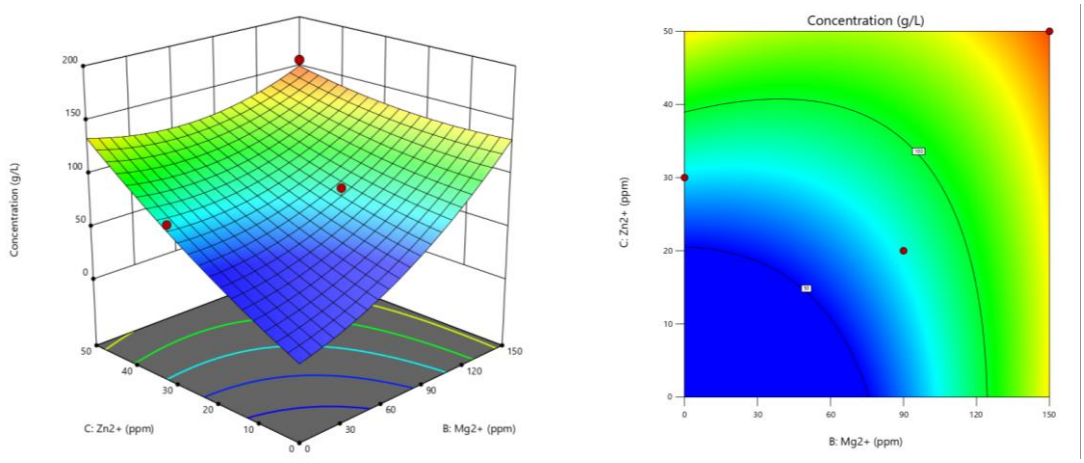

(a) (b)

Figure 4. Response surface for the addition of Zn^{2+} and Mg^{2+} ions on bioethanol concentration.

The response surface plots and contour plots presented in Figures 2 through 4 illustrate the complex, multivariate interactions between the concentrations of Ca^{2+}, Mg^{2+}, and Zn^{2+} ions, and their effect on bioethanol production. The three-dimensional surface plots demonstrate a nonlinear relationship between the ion concentrations and the resultant bioethanol concentration. Specifically, Figure 2 indicates a positive correlation between the concentrations of Ca^{2+} and

Mg^{2+}, with an optimal bioethanol content achieved at approximately 100–150 ppm for Ca^{2+} and 150 ppm for Mg^{2+}. This optimal combination is further substantiated by the experimental results from Run 3, where the bioethanol concentration reached 156.58 g/L. Similarly, Figure 3 demonstrates that the highest bioethanol concentration is obtained with a combination of 200 ppm Ca^{2+} and 20–50 ppm Zn^{2+}, as evidenced by Run 9, which produced a concentration of 158.31 g/L. In contrast, the interaction between Mg^{2+} and Zn^{2+}, as depicted in Figure 4, also shows a positive influence on bioethanol production, but the magnitude of the response is less pronounced compared to the Ca^{2+} and Zn^{2+} interaction. The data from these response surface plots and corresponding contour plots suggest that there exists a precise range of ion concentrations that facilitates the maximization of bioethanol production.

3.5. Optimization of Bioethanol Production Process with the Addition of Ca^{2+}, Mg^{2+}, and Zn^{2+} Ions

Table 7. Results of bioethanol production optimization the addition of Ca^{2+}, Mg^{2+}, and Zn^{2+} ions.

Number	Ca^{2+}	Mg^{2+}	Zn^{2+}	Concentration	EtOH Content	Desirability
1	**194.691**	**144.398**	**39.429**	**178.664**	**18.461**	**1.000**
2	199.947	94.339	49.874	166.363	17.170	1.000
3	194.517	149.814	27.722	165.371	17.067	1.000
4	194.271	144.652	32.081	165.901	17.125	1.000
5	122.275	147.681	48.577	159.568	16.454	1.000

The experimental results presented in Table 7 demonstrate the optimization of bioethanol production with the addition of Ca^{2+}, Mg^{2+}, and Zn^{2+} ions. Each combination of ion concentrations tested produced a desirability value of 1, signifying successful enhancement of bioethanol production. The concentrations of Ca^{2+}, Mg^{2+}, and Zn^{2+} ions, along with their respective ethanol content and desirability values, are outlined in the table 7. For instance, in Experiment 1, the concentrations of Ca^{2+} (194.691 mg/L), Mg^{2+} (144.398 mg/L), and Zn^{2+} (39.429 mg/L) resulted in a bioethanol concentration of 18.461 mg/L, with a desirability of 1. While the ethanol content fluctuated across the experiments, all combinations reached the same desirability value of 1, indicating that each combination successfully optimized bioethanol production under the given conditions [26].

4. Conclusion

The presence of ions such as Ca^{2+}, Mg^{2+}, and Zn^{2+} plays a significant role in the fermentation process that produces bioethanol. Based on the experiment and optimization analysis, it can be concluded that the production of bioethanol is significantly influenced by the concentrations of Ca^{2+}, Mg^{2+}, and Zn^{2+} ions. The optimal concentrations for maximizing bioethanol content and concentration were identified as 164.755 ppm for Ca^{2+}, 146.279 ppm for Mg^{2+}, and 38.516 ppm for Zn^{2+}, which resulted in a bioethanol content of 17.087% and a final concentration of 165.592 g/L. Addition of Ca^{2+} ion enhanced the stability and metabolic activity of Saccharomyces cerevisiae cells, leading to increased ethanol production, while the supplementation of Mg^{2+} and Zn^{2+} ions improved fermentation efficiency and sugar-to-ethanol conversion. In the present study, the highest bioethanol concentrations were achieved in runs where Mg^{2+} was supplemented in optimal concentrations, in combination with Ca^{2+} and Zn^{2+}. While Zn^{2+} ions played a supporting role in enzymatic activity and cell viability, their excessive concentration did not significantly improve bioethanol production. These values were derived through Response Surface Methodology (RSM), which facilitated the determination of the optimal ion concentrations that yield the highest bioethanol production. The statistical analysis of the data, including the high coefficient of determination ($R^2 = 0.9993$), confirmed the robustness and predictive power of the model. The results underscore the critical role of Mg^{2+} ions in enhancing fermentation efficiency, particularly in combination with Ca^{2+} and Zn^{2+}. This study provides a comprehensive understanding of the interactions between these ions and their effect on bioethanol production, offering valuable insights for optimizing industrial fermentation processes.

Acknowledgment

The author would like to show gratitude to the Department of Industrial Chemical Engineering, Vocational Faculty, Institut Teknologi Sepuluh Nopember (ITS) for support provided throughout this research.

References

[1] N. Jeyakumar *et al.*, "Experimental investigation on simultaneous production of bioethanol and biodiesel from macro-algae," *Fuel*, vol. 329, p. 125362, Dec. 2022, doi: 10.1016/j.fuel.2022.125362.

[2] M. V. Rodionova *et al.*, "Biofuel production: Challenges and opportunities," *Int J Hydrogen Energy*, vol. 42, no. 12, pp. 8450–8461, Mar. 2017, doi: 10.1016/j.ijhydene.2016.11.125.

[3] S. Soeprijanto, L. Qomariyah, A. Hamzah, and S. Altway, "Bioconversion of Industrial Cassava Solid Waste (Onggok) to Bioethanol Using a Saccharification and Fermentation process," *International Journal of Renewable Energy Development*, vol. 11, no. 2, pp. 357–363, May 2022, doi: 10.14710/ijred.2022.41332.

[4] A. T. Hoang *et al.*, "Catalyst-Based Synthesis of 2,5-Dimethylfuran from Carbohydrates as a Sustainable Biofuel Production Route," *ACS Sustain Chem Eng*, vol. 10, no. 10, pp. 3079–3115, Mar. 2022, doi: 10.1021/acssuschemeng.1c06363.

[5] P. Ranganathan, A. K. Pandey, R. Sirohi, A. Tuan Hoang, and S.-H. Kim, "Recent advances in computational fluid dynamics (CFD) modelling of photobioreactors: Design and applications," *Bioresour Technol*, vol. 350, p. 126920, Apr. 2022, doi: 10.1016/j.biortech.2022.126920.

[6] R. Maryana *et al.*, "Bioethanol production process with SHF method from EFBs pulp and its microcrystalline," *IOP Conf Ser Earth Environ Sci*, vol. 1108, no. 1, p. 012021, Nov. 2022, doi: 10.1088/1755-1315/1108/1/012021.

[7] T. J. Tse, D. J. Wiens, and M. J. T. Reaney, "Production of Bioethanol—A Review of Factors Affecting Ethanol Yield," *Fermentation*, vol. 7, no. 4, p. 268, Nov. 2021, doi: 10.3390/fermentation7040268.

[8] T. Kandungan *et al.*, "Pengaruh Penambahan Ion Mg 2+."

[9] E. Demiray, S. E. Karatay, and G. Dönmez, "Evaluation of pomegranate peel in ethanol production by Saccharomyces cerevisiae and Pichia stipitis," *Energy*, vol. 159, pp. 988–994, Sep. 2018, doi: 10.1016/j.energy.2018.06.200.

[10] O. K. Agwa, I. G. Nwosu, and G. O. Abu, "Bioethanol Production from <i>Chlorella vulgaris</i> Biomass Cultivated with Plantain (<i>Musa paradisiaca</i>) Peels Extract," *Advances in Bioscience and Biotechnology*, vol. 08, no. 12, pp. 478–490, 2017, doi: 10.4236/abb.2017.812035.

[11] E. Hawaz *et al.*, "Bioethanol production from sugarcane molasses by co-fermentation of Saccharomyces cerevisiae isolate TA2 and Wickerhamomyces anomalus isolate HCJ2F-19," *Ann Microbiol*, vol. 74, no. 1, p. 13, Apr. 2024, doi: 10.1186/s13213-024-01757-8.

[12] F. M. Alminderej, Z. Hamden, Y. El-Ghoul, B. Hammami, S. M. Saleh, and H. Majdoub, "Impact of Calcium and Nitrogen Addition on Bioethanol Production by S. cerevisiae Fermentation from Date By-Products: Physicochemical Characterization and Technical Design," *Fermentation*, vol. 8, no. 11, p. 583, Oct. 2022, doi: 10.3390/fermentation8110583.

[13] A. Kevin Santoso, A. Livia Hidayat, A. Rexer Fransenda, A. Hasiholan Marpaung, and S. Glory Sihombing, "Optimizing Bioethanol Production through Separated Hydrolysis Fermentation of Rubber-Cassava (Manihot Glaziovii) Starch with K + and Mg 2+ Mineral Ion Supplements," 2023. [Online]. Available: www.ijisrt.com

[14] C. Wan *et al.*, "The impact of zinc sulfate addition on the dynamic metabolic profiling of Saccharomyces cerevisiae subjected to long term acetic acid stress treatment and identification of key metabolites involved in the antioxidant effect of zinc," *Metallomics*, vol. 7, no. 2, pp. 322–332, 2015, doi: 10.1039/C4MT00275J.

[15] R. Barros de Souza, R. K. Silva, D. S. Ferreira, S. de Sá Leitão Paiva Junior, W. de Barros Pita, and M. A. de Morais Junior, "Magnesium ions in yeast: setting free the metabolism from glucose catabolite repression," *Metallomics*, vol. 8, no. 11, pp. 1193–1203, 2016, doi: 10.1039/C6MT00157B.

[16] D. Fiorentini, C. Cappadone, G. Farruggia, and C. Prata, "Magnesium: Biochemistry, Nutrition, Detection, and Social Impact of Diseases Linked to Its Deficiency," *Nutrients*, vol. 13, no. 4, p. 1136, Mar. 2021, doi: 10.3390/nu13041136.

[17] S. Chotineeranat, R. Wansuksri, K. Piyachomkwan, P. Chatakanonda, P. Weerathaworn, and K. Sriroth, "Effect of calcium ions on ethanol production from molasses by Saccharomyces cerevisiae," *Sugar Tech*, vol. 12, no. 2, pp. 120–124, Jun. 2010, doi: 10.1007/s12355-010-0024-6.

[18] J. R. Robinson, O. S. Isikhuemhen, and F. N. Anike, "Fungal–Metal Interactions: A Review of Toxicity and Homeostasis," *Journal of Fungi*, vol. 7, no. 3, p. 225, Mar. 2021, doi: 10.3390/jof7030225.

[19] Syaputri, F. Panca, and D. Salirawati, "PENGARUH ION LOGAM Zn2+ DALAM BENTUK SENYAWA ZnSO4 TERHADAP AKTIVITAS ENZIM α-AMILASE," *Jurnal Elemen Kimia*, vol. 8, no. 1, pp. 1–7, 2024.

[20] T. A. Mekuriaw and M. K. Abera, "<math altimg="si1.svg"> <mrow> <mtext>CaO</mtext> </mrow> </math> -catalyzed trans-esterification of brassica carinata seed oil for biodiesel production," *Heliyon*, vol. 10, no. 13, p. e33790, Jul. 2024, doi: 10.1016/j.heliyon.2024.e33790.

[21] S. Altınışık, F. U. Nigiz, S. Gürdal, K. Yılmaz, N. B. Tuncel, and S. Koyuncu, "Optimization of bioethanol production from sugar beet processing by-product molasses using response surface methodology," *Biomass Convers Biorefin*, vol. 15, no. 7, pp. 9875–9888, Apr. 2025, doi: 10.1007/s13399-024-05786-w.

[22] M. Pirsaheb *et al.*, "Preparation of the activated carbon from India shrub wood and their application for methylene blue removal: modeling and optimization," *Desalination Water Treat*, vol. 57, no. 13, pp. 5888–5902, Mar. 2016, doi: 10.1080/19443994.2015.1008581.

[23] T. Tadesse, D. Dase, A. D. Koricha, and K. Bacha, "Optimization of Bioethanol Production Using Response Surface Methodology for Stress-Tolerant Wild Yeasts Isolated from Natural Forests," *Int J Energy Res*, vol. 2024, no. 1, Jan. 2024, doi: 10.1155/2024/7086047.

[24] M. Yolmeh and S. M. Jafari, "Applications of Response Surface Methodology in the Food Industry Processes," *Food Bioproc Tech*, vol. 10, no. 3, pp. 413–433, Mar. 2017, doi: 10.1007/s11947-016-1855-2.

[25] L. M. S. Pereira, T. M. Milan, and D. R. Tapia-Blácido, "Using Response Surface Methodology (RSM) to optimize 2G bioethanol production: A review," *Biomass Bioenergy*, vol. 151, p. 106166, Aug. 2021, doi: 10.1016/j.biombioe.2021.106166.

[26] M. Sarah, I. Madinah, E. Misran, and Fatimah, "Optimization of microwave-assisted hydrolysis of glucose from oil palm empty fruit bunch," *S Afr J Chem Eng*, vol. 51, pp. 1–14, Jan. 2025, doi: 10.1016/j.sajce.2024.10.004.